Published in final edited form as:
J Mol Histol. 2011 February ; 42(1): 3–13. doi:10.1007/s10735-010-9302-6.

Characterization of basal pseudopod-like processes in ileal and colonic PYY cells

Diego V. Bohórquez,
Department of Medicine, Duke University, Durham, NC, USAVeterans Affairs Medical Center, Durham, NC 27710, USA

Rashmi Chandra,
Department of Medicine, Duke University, Durham, NC, USAVeterans Affairs Medical Center, Durham, NC 27710, USA

Leigh Ann Samsa,
Department of Medicine, Duke University, Durham, NC, USAVeterans Affairs Medical Center, Durham, NC 27710, USA

Steven R. Vigna, and
Department of Medicine, Duke University, Durham, NC, USAVeterans Affairs Medical Center, Durham, NC 27710, USA

Rodger A. Liddle
Department of Medicine, Duke University, Durham, NC, USA. Veterans Affairs Medical Center, Durham, NC 27710, USA. Duke University Medical Center, Box 3913, Durham, NC 27707, USA

Rodger A. Liddle: liddl001@mc.duke.edu

Abstract

The peptide tyrosine tyrosine (PYY) is produced and secreted from L cells of the gastrointestinal mucosa. To study the anatomy and function of PYY-secreting L cells, we developed a transgenic PYY-green fluorescent protein mouse model. PYY-containing cells exhibited green fluorescence under UV light and were immunoreactive to antibodies against PYY and GLP-1 (glucagon-like peptide-1, an incretin hormone also secreted by L cells). PYY-GFP cells from 15 μm thick sections were imaged using confocal laser scanning microscopy and three-dimensionally (3D) reconstructed. Results revealed unique details of the anatomical differences between ileal and colonic PYY-GFP cells. In ileal villi, the apical portion of PYY cells makes minimal contact with the lumen of the gut. Long pseudopod-like basal processes extend from these cells and form an interface between the mucosal epithelium and the lamina propria. Some basal processes are up to 50 μm in length. Multiple processes can be seen protruding from one cell and these often have a terminus resembling a synapse that appears to interact with neighboring cells. In colonic crypts, PYY-GFP cells adopt a spindle-like shape and weave in between epithelial cells, while maintaining contact with the lumen and lamina propria. In both tissues, cytoplasmic granules

Correspondence to: Rodger A. Liddle, liddl001@mc.duke.edu.

Drs. Bohórquez and Chandra contributed equally to this work and should be considered co-first authors.

containing the hormones PYY and GLP-1 are confined to the base of the cell, often filling the basal process. The anatomical arrangement of these structures suggests a dual function as a dock for receptors to survey absorbed nutrients and as a launching platform for hormone secretion in a paracrine fashion.

Keywords

L cell; Confocal microscopy; Peptide YY; Green fluorescent protein; Pseudopod

Introduction

The hormone peptide tyrosine tyrosine (PYY) has been at the forefront of obesity research based on its ability to induce satiety and produce weight loss (Field et al. 2010). PYY is synthesized as a 36 amino acid peptide ($PYY_{1–36}$) that is processed to a shorter form ($PYY_{3–36}$), which potently decreases appetite and reduces weight gain when administered intravenously at physiological levels (Batterham et al. 2002). The L cells of the gastrointestinal mucosa secrete PYY in response to lipids (Greeley Jr et al. 1989) and amino acids and proteins (Zhang et al. 1993; Batterham et al. 2006) present in the lumen of the gut. Besides being a major signal of satiety, circulating PYY has been shown to inhibit esophageal muscle contraction (Huang 2000), delay gastric emptying (Savage et al. 1987), inhibit jejunal and colonic motility (Lundberg et al. 1982), act as a vasoconstrictor (Lundberg et al. 1982), and regulate renal sodium excretion (Playford et al. 1995). While most of the attention has been focused on the physiological effects of this hormone, relatively little is known about the biology of the PYY-secreting L cell. In 1982, Lundberg et al. noticed that PYY immunoreactive cells occasionally had long processes extending at their basal portion. However, the anatomy and function of these structures in the L cell has yet to be described.

The study of these basal processes has been limited by the fact that PYY antibodies bind primarily to granules containing the hormone and do not delineate the entire contour of the cell. Recently, Chandra et al. (2010) used a transgenic CCK-green fluorescent protein (GFP) mouse model to describe the structure of pseudopod-like basal cell processes in intestinal cholecystokinin (CCK) cells. When combined with confocal laser scanning microscopy (CLSM), this model allowed for a detailed three-dimensional reconstruction of GFP-positive cells. Hence, we developed in our lab a transgenic PYY-GFP mouse model to study PYY-secreting cells. During the course of this work, we noticed that the anatomy of GFP-positive cells and their basal processes vary depending on their location along the intestinal tract. Moreover, the terminal end of the basal processes often resembles a synapse that appears to interact with other cells nearby. Therefore, the aim of the present report was to describe the morphological characteristics of basal processes in ileal and colonic PYY cells.

Materials and methods

Generation of transgenic PYY-GFP mouse

Bacteria artificial chromosome (BAC) clones, RP23-291A19 and RP23-218N17, were obtained from the BAC resource center at the Children's Hospital Oakland Research Institute (Oakland, CA, USA). Clones were characterized by restriction enzyme digests run on pulse field gels and PCR. An enhanced GFP DNA fragment was amplified from pEGFP-N1 (Clontech Laboratories, Inc. Mountain View, CA, USA) and the BGH polyadenylation sequence was amplified from pcDNA3.1 (Invitrogen Corporation, Carlsbad, CA, USA). The two PCR products were joined by recombinant PCR (Higuchi 1990), and the EGFP-BGH sequence was cloned into a pBluescript KS plasmid and transformed into XL1 bacteria (Agilent Technologies, Santa Clara, CA, USA). DNA from two bacterial colonies (pEGFP-BGH/pBS) was sequenced in its entirety to identify clones with no base pair errors. Subsequently, a neomycin cassette FRT-Neo/Kan-FRT sequence was amplified by PCR from the pIGCN21 plasmid (Lee et al. 2001). The PCR product was digested with the appropriate restriction enzymes and cloned downstream of the EGFP-BGH sequence in EGFP-BGH/pBS. Homologous PYY arms were then amplified and cloned into this vector as follows: 895 base pairs (bp) of PYY sequence directly upstream of the start codon (A box) and 681 bp of PYY sequence directly downstream of the stop codon (B box). The A box was cloned upstream of the EGFP-BGH sequence and the B box was cloned downstream of the FRT-Neo/Kan-FRT cassette. All PCR amplified DNA was sequenced in its entirety on both strands. The PYY targeting fragment cut 5′ of the A-Box and 3′ of the B-Box was purified from the pBluescript plasmid.

BAC DNA was purified from DH10B bacterial cells and transformed into SW105 bacteria. The BAC DNA from SW105 cells was characterized by restriction digests run on pulse field gels and PCR (of the PYY region) to verify the integrity of the BAC. The PYY targeting fragment was then electroporated into BAC-containing SW105 cells induced for recombination by a temperature shift to 42°C for 15 min. Recombined BACs were selected with antibiotics and the neomycin cassette was removed by arabinose induction of flipase expression. Recombined and neo excised clones were again characterized by restriction digests on pulse field gels and PCR. Verified BACs were transferred to the Duke University Neurotransgenics Facility, where BACs were linearized by Asc I and gel purified. After filter dialysis, the BAC DNA concentration was adjusted to 1 ng/μl and microinjected into the pronuclei of B6SJF1 mouse oocytes. Two independent founder lines of PYY-GFP transgenic mice were generated; both founders were derived from the EGFP construct cloned into the RP23-218N17 BAC.

The founder lines were bred in house at the Division of Laboratory Animal Resources of Duke University School of Medicine. Animals were raised in a 12 h light–12 h dark cycle and had *ad libitum* access to feed and water. Animal care and experiments were carried out in accordance with a protocol approved by the Institutional Animal Care and Use Committee of Duke University Medical Center.

Tissue collection

Tissue harvesting and PYY immunofluorescence were carried out as described previously by Chandra et al. (2010), with some modifications. Eight- to twelve-week-old mice were anesthetized with a mixture of ketamine and xylazine and perfused intracardially with ice-cold, freshly depolymerized 3.5% paraformaldehyde (PFA) in phosphate buffered saline (PBS, pH 7.4). Five centimeters of the distal ileum (adjacent to the ileo-cecal junction) as well as the entire colon (from the cecal junction to the anal canal) were removed, flushed with PBS, and fixed in PFA for 3 h at 4°C. Tissues were cryo-protected sequentially in cold 10 and 20% sucrose in PBS, then incubated overnight at 4°C in 30% sucrose. The next day, smaller sections (~1 cm) were embedded in molds containing Tissue-Tek OCT compound (Sakura Finetek, Torrance, CA, USA) and rapidly frozen on dry ice for cryosectioning. Sections (15 μm thick) were cut using a cryostat and mounted on positively charged microscope slides (Globe Scientific Inc., Paramus, NJ). The use of sections at least 15 μm thick was critical for three-dimensional reconstruction of cells in the tissue. Slides were air dried at room temperature for at least 1 h before being stored at −80°C.

PYY immunofluorescence

Antibodies used, suppliers, and antibody-specific staining conditions are listed on Table 1. The PYY antibody was raised in rabbits using a synthetic peptide, KPEAPGE-DASPEELSRYC, corresponding to amino acids 4–21 of mouse PYY, affinity-purified and characterized in our laboratory. In general, slides were thawed at room temperature for 30 min and post-fixed in 10% neutral buffered formalin (NBF) for 10 min (4°C). They were then washed in 50 mM TRIS buffered saline containing 0.05% Tween-20 (TBST) three times (5 min each). All washes from this point forward were performed under the same conditions unless otherwise stated. Non-specific binding was blocked by incubation with 10% normal donkey serum in PBS for 30 min. The serum was removed and sections were incubated with the primary rabbit PYY antibody for 1 h. Slides were washed and sections were incubated with the appropriate secondary antibody for 1 h. Finally, slides were washed and counter-stained with 300 nM DAPI (Invitrogen Corporation, Carlsbad, CA, USA). Cover slips (# 1.5) were mounted using Prolong Gold anti-fade reagent (Invitrogen Corporation, Carlsbad CA, USA). Control sections included: a) wild-type mouse tissues treated with PYY antibody to show PYY immunoreactive cells in their native form; b) transgenic PYY-GFP mouse tissues treated with secondary antibody alone to control for non-specific binding; and c) transgenic PYY-GFP mouse tissues treated with PYY antibody that was previously pre-adsorbed (24 h at 4°C) in 10 μM of PYY synthetic peptide to test for the specificity of the antibody. Images from controls are presented in Fig. 1.

PYY and GLP-1 immunofluorescence

We used Tyramide Signal Amplification™ (TSA™, PerkinElmer, Waltham, MA, USA) to localize PYY and GLP-1 in GFP-positive cells because the available antibodies were both raised in rabbits. This method has been previously reported for detection of peptides using antibodies raised in the same species (Liu et al. 2006; Shindler and Roth 1996). Table 2 contains a description of the antibodies used, their source and incubation conditions for TSA™ amplification. Briefly, sections (15 μm thick) were post-fixed in 10% NBF for 10

min (4°C). They were then incubated in 0.02 N HCl for 10 min to quench endogenous peroxidase activity. Slides were washed and sections were blocked for 1 h with normal donkey serum (1:10 in PBS), followed by an overnight incubation (4°C) with the first primary antibody (rabbit anti-PYY) at a dilution only detectable by TSA™ amplification. Sections were washed, incubated for 1 h with peroxidase-conjugated anti-rabbit secondary antibody, washed again and incubated for 20 min with TAS™-Cy5 amplifying reagent. Sections were then washed and incubated for 1 h with the second primary antibody (rabbit anti-GLP-1) and a chicken antibody against GFP. The GFP antibody was introduced to prolong the duration of GFP signal while imaging a series of Z-stacks. Slides were washed and sections were incubated for 1 h with secondary antibodies anti-rabbit IgG conjugated to Cy3 and anti-chicken IgG conjugated to Dylight488. Finally, slides were washed, counterstained with DAPI, and cover slips were mounted using mounting Prolong Gold anti-fade reagent. Controls included sections treated with rabbit anti-PYY and/or rabbit anti-GLP-1 without secondary antibody and sections treated with secondary antibody alone.

Image acquisition and analysis

Samples were imaged on a Zeiss 510 inverted confocal microscope using 20X/0.8 (Zeiss Plan Apochromat), 40X/1.3 (Zeiss Plan NeoFluar) or 100X/1.4oil (Zeiss Plan Apochromat) objectives. Single optical sections or Z-stacks were obtained using sequential multi-track acquisition with excitation at 405 (DAPI), 488 (eGFP or DyLight 488), 561 (Cy3), and 633 nm (TAS™-Cy5), and emission filters of BP 420–480, BP505–550, LP575, and LP650. Pinholes were set to 1 airy unit and line averaging of 8 at 1,024 pixel resolution. Differential interference contrast (DIC) images were also collected to determine the location of the cells relative to the lumen. To visualize the images in 3D, Z-stacks were deconvolved using Huygens® Essential software (BioVision Technologies, Exton, PA, USA) and reconstructed in 3D using Volocity® (PerkinElmer, Waltham, MA, USA). Channels were visualized as: maximum intensity projections (green/GFP, red/PYY, cyan/GLP-1), which allow the channel's color to be seen through other channels or as fluorescence (blue/DAPI).

Results

Cells expressing enhanced GFP (eGFP), driven by the PYY promoter, were immunoreactive with an antibody specific to PYY (Fig. 1). Moreover, triple immunofluorescence staining for PYY, GLP-1, and GFP revealed colocalization of PYY and GLP-1 within GFP-positive cells (Fig. 2). PYY-GFP cells were observed from the pyloric region of the gastric mucosa to the distal descending colon (data not shown), though the vast majority were found in the distal ileum and colon (Fig. 3). In both, the ileum and colon, GFP-PYY cells were more abundant at the bottom of the crypts than at the apex of the mucosa (e.g., villi in the ileum). GFP expression was visible at around cell position #3 counting from the bottom of the crypt. In this position in both the ileum and colon, PYY-GFP cells were columnar in shape and basal processes were short or absent (Fig. 4). However, as the cells were observed further up from the crypt base, their cell bodies adopted a flask-shape with a long pseudopod-like structure extending from the bottom of the cell (Fig. 4). From this point in the crypts, there appeared unique anatomical differences between ileal and colonic PYY-GFP cells.

PYY-GFP cells in the ileum had at least one process that almost invariably extended from the cell base down toward the bottom of the crypt (Figs. 4 and 5). Processes appeared to form an interface between the base of the columnar epithelial cells and the lamina propria. Some cells were over 70 μm long with a basal process that reached up to 50 μm in length (Fig. 5). Many PYY-GFP cells had more than one process (Fig. 6). The additional processes were often visible at the base of the cell and extended away from the direction of the crypt. Other processes were observed protruding from the body of the cell towards other epithelial cells (Fig. 6). Interestingly, the distal ends of some processes resembled a synapse (Fig. 5e and 6). Occasionally, such endings appeared to interact with unidentified structures below the basal lamina and with other GFP-positive cells in the epithelium (Fig. 6). However, they also were found extending to GFP-negative epithelial cells.

In the colon, PYY-GFP cells at the apex of crypts exhibited a spindle-like shape and their basal processes were found in between other epithelial cells (Fig. 4). In this way, one PYY-GFP cell can span more than 15 epithelial cells lengthwise and still be exposed to the lumen of the crypt and lamina propria at the same time (Fig. 7). Despite the fact that the synapse-like endings appeared to be absent in colonic PYY-GFP cells, some bifurcations were observed but were fewer than those seen in the ileum (data not shown).

Discussion

PYY has received recent attention in obesity research because of its abilities to induce satiety and weight loss in rodents and humans (Batterham et al. 2002; Batterham et al. 2006). Although some of the effects of circulating PYY have been well documented, relatively little is known about the biology of the PYY-secreting L cell. Here we report the use of a transgenic PYY-GFP mouse to study PYY cell anatomy in the distal gastrointestinal tract. In agreement with previous reports on the localization of PYY cells (El-Salhy et al. 1983), PYY-GFP cells were found distributed along the gastrointestinal mucosa, predominantly in the ileum and colon. GFP-positive cells were immunoreactive with PYY and GLP-1 antibodies, which is typical of enteroendocrine L cells (Nilsson et al. 1991). Cells expressing eGFP occasionally did not colocalize with PYY antiserum, perhaps because eGFP can bleach during the staining process and while imaging. To avoid such an artifact, we used a chicken polyclonal antibody against GFP (cGFP) previously described by Chandra et al. (2010). Staining with cGFP clearly delineated the contour of PYY cells and allowed enhanced visualization of their anatomical characteristics.

PYY cells in the ileum appeared anatomically different than those in the colon. The main difference is that mature ileal PYY cells have a classic L-shape, whereas mature colonic cells have a spindle- or sigmoidal-like contour. In the ileum, the apical portion of these cells maintains minimal contact with the gut lumen whereas in the colon the contact with the lumen appears more prominent. PYY cells in both the ileum and the colon have a long basal process running underneath other epithelial cells. Although the existence of basal processes in PYY cells has been recognized for decades (Lundberg et al. 1982; Karaki et al. 2006), no anatomical or functional description of these structures has been reported. Studies in somatostatin cells have suggested that these anatomical adaptations help to direct the paracrine secretion of somatostatin onto neighboring gastrin cells (Alumets et al. 1979). In

this way, somatostatin cells in the stomach can regulate gastrin and hydrochloric acid secretion. Interestingly, basal processes in somatostatin cells have been described to end in bulb-like swellings (Alumets et al. 1979). Our results also indicate that the processes in PYYGFP cells end in bulb-like swellings that resemble synapses. We have co-immunostained PYY-GFP sections with markers for neuroendocrine (chromogranin A), goblet (intestinal trefoil-factor-3) and enterochromaffin-like cells (serotonin) and these cell types do not appear to be specific targets of the PYY-GFP processes (data not shown). However, Wade and Westfall (1985) have reported using electron microscopy that basal processes in putative enteroendocrine cells are in close proximity to neurites located below the basal lamina. Therefore, basal processes in PYY-secreting cells may target specific cell types located in the lamina propria.

Quantitative receptor autoradiography and immunohistochemical studies have demonstrated the existence of PYY receptors in the mucosa of the distal colon (Mannon et al. 1993; Jackerott and Larsson 1997; Mannon et al. 1999). Hence, secreted PYY most likely influences adjacent cells in a paracrine fashion. Electron microscopy and immunohistochemical studies have shown that enteroendocrine cells including L cells, harbor their secretory granules at their base (Cheng and Leblond 1974; Lundberg et al. 1982). In agreement, our images showed that PYY immunoreactivity is almost exclusively confined to the basal processes of GFP-positive cells (Fig. 4). Moreover, triple immuno-fluorescence staining with antibodies against GFP, PYY, and GLP-1 revealed that both PYY and GLP-1 granules are located at the basal end of GFP-positive cells (Fig. 2). Feinle-Bisset et al. (2005) have shown that digestion of ingested fats is necessary for lipid-mediated PYY secretion. Hence, PYY secretion is likely mediated by receptors activated by specific types of lipids. Recently, short chain fatty acid receptors (e.g. GPR41, GPR43, GPR119) have been shown to colocalize with PYY-secreting cells in humans and rodents (Karaki et al. 2008; Karaki et al. 2006; Coxsend et al. 2010). Moreover, the staining for these receptors appears to be confined to the basal portion of PYY cells (Karaki et al. 2008; Karaki et al. 2006). Hence, PYY cell processes may serve a dual function: (1) as an anchor for receptors to survey the passage of absorbed nutrients at the base of enterocytes, and (2) as a launching platform to direct the secretion of PYY into the bloodstream, neighboring cells or specific targets in the lamina propria. However, the specific functions and dynamics of these structures remains to be elucidated.

In summary, the use of a transgenic PYY-GFP mouse model provides unique anatomical details of the PYY-secreting L cell, which are depicted in Fig. 7. GFP-positive cells contained PYY and GLP-1, typical of the enteroendocrine L cell. The majority of PYY immunoreactivity was colocalized at the base of the cells, often filling the basal process. In the ileum, these cells had long extending basal processes with terminal endings that resemble synapses. More than one process could be observed protruding from the body of the same cell. In the colon, the cells at the apex of the crypt had a spindle-like shape that wove in between epithelial cells while maintaining contact with both the lumen and lamina propria. The unique anatomy and location of the basal process in PYY-secreting cells may serve to survey nutrient absorption and secrete hormone in an endocrine and paracrine fashion.

Acknowledgments

We thank Drs. Samuel Johnson and Yasheng Gao from the Light Microscopy Core Facility at Duke University for their valuable assistance with confocal microscopy. This work was supported by National Institutes of Health grant DK38626.

References

Alumets J, Ekelund M, Munshid H, HÂkanson R, Loren I, Sundler F. Topography of somatostatin cells in the stomach of the rat: possible functional significance. Cell Tiss Res. 1979; 202:177–188.

Batterham R, Cowley M, Small C, Herzog H, Cohen M, Dakin C, Wren A, Brynes A, Low M, Ghatei M. Gut hormone PYY3–36 physiologically inhibits food intake. Nature. 2002; 418:650–654. [PubMed: 12167864]

Batterham R, Heffron H, Kapoor S, Chivers J, Chandarana K, Herzog H, Le Roux C, Thomas E, Bell J, Withers D. Critical role for peptide YY in protein-mediated satiation and body-weight regulation. Cell Metabol. 2006; 4:223–233.

Chandra R, Samsa L, Vigna S, Liddle R. Pseudopod-like basal cell processes in intestinal cholecystokinin cells. Cell Tiss Res. 201010.1007/s00441-010-0997-1

Cheng H, Leblond CP. Origin, differentiation and renewal of the four main epithelial cell types in the mouse small intestine III. Entero-endocrine cells. Am J Anat. 1974; 141:503–519. [PubMed: 4216261]

Coxsend H, Tough I, Woolston A, Zhang L, Nguyen A, Sainsbury A, Herzog H. Peptide YY is critical for acylethanolamine receptor GPR119-induced activation of gastrointestinal mucosal responses. Cell Metabol. 2010; 11:532–542.

El-Salhy M, Wilander E, Juntti-Berggren L, Grimelius L. The distribution and ontogeny of polypeptide YY (PYY)-and pancreatic polypeptide (PP)-immunoreactive cells in the gastrointestinal tract of rat. Histochem Cell Biol. 1983; 78:53–60.

Feinle-Bisset C, Patterson M, Ghatei M, Bloom S, Horowitz M. Fat digestion is required for suppression of ghrelin and stimulation of peptide YY and pancreatic polypeptide secretion by intraduodenal lipid. Am J Physiol Endocrinol Metabol. 2005; 289:E948–E953.10.1152/ajpendo.00220.20050193-1849

Field B, Chaudhri O, Bloom S. Bowels control brain: gut hormones and obesity. Nature Rev Endocrinol. 2010; 6:444–453. [PubMed: 20585346]

Greeley G Jr, Hashimoto T, Izukura M, Gomez G, Jeng J, Hill F, Lluis F, Thompson J. A comparison of intraduodenally and intracolonically administered nutrients on the release of peptide-YY in the dog. Endocrinology. 1989; 125:1761–1765. [PubMed: 2791964]

Higuchi, R. Recombinant pcr. In: Innis, M.; Gelfand, D.; Sninsky, J.; White, T., editors. PCR protocols: a guide to methods and applications. Academic Press, Inc; San Diego: 1990. p. 177-183.

Huang S. Functional CCK-a and Y2 receptors in guinea pig esophagus. Regul Peptides. 2000; 88:55–60.

Jackerott M, Larsson L. Immunocytochemical localization of the NPY/PYY Y1 receptor in enteric neurons, endothelial cells, and endocrine-like cells of the rat intestinal tract. J Histochem Cytochem. 1997; 45:1643. [PubMed: 9389767]

Karaki S, Mitsui R, Hayashi H, Kato I, Sugiya H, Iwanaga T, Furness J, Kuwahara A. Short-chain fatty acid receptor, GPR43, is expressed by enteroendocrine cells and mucosal mast cells in rat intestine. Cell Tiss Res. 2006; 324:353–360.

Karaki S, Tazoe H, Hayashi H, Kashiwabara H, Tooyama K, Suzuki Y, Kuwahara A. Expression of the short-chain fatty acid receptor, GPR43, in the human colon. J Mol Histol. 2008; 39:135–142. [PubMed: 17899402]

Lee E, Yu D, de Valasco M, Tessarollo L, Swing D, Court D, Jenkins N, Copeland N. A highly efficient *Escherichia coli*-based chromosome engineering system adapted for recombinogenic targeting and subcloning of BAC DNA. Genomics. 2001; 73:56–65. [PubMed: 11352566]

Liu G, Amin S, Okuhama N, Liao G, Mingle L. A quantitative evaluation of peroxidase inhibitors for tyramide signal amplifi-cation mediated cytochemistry and histochemistry. Histochem Cell Biol. 2006; 126:283–291. [PubMed: 16508759]

Lundberg J, Tatemoto K, Terenius L, Hellstřm P, Mutt V, Ůkfelt T, Hamberger B. Localization of peptide YY (PYY) in gastrointestinal endocrine cells and effects on intestinal blood flow and motility. Proc Nat Acad Sci. 1982; 79:4471–4475. [PubMed: 6956876]

Mannon P, Hernandez E, Mervin S, Vigna S, Taylor I. Characterization of peptide YY receptors in rabbit colonic mucosa. Peptides. 1993; 14:567–572. [PubMed: 8392723]

Mannon P, Kanungo A, Mannon R, Ludwig K. Peptide YY/neuropeptide Y Y1 receptor expression in the epithelium and mucosal nerves of the human colon. Regul Peptides. 1999; 83(1):11–19.

Nilsson O, Bilchik A, Goldenring J, Ballantyne G, Adrian T, Modlin I. Distribution and immunocytochemical colocalization of peptide YY and enteroglucagon in endocrine cells of the rabbit colon. Endocrinology. 1991; 129(1):139–148. [PubMed: 1675986]

Playford R, Mehta S, Upton P, Rentch R, Moss S, Calam J, Bloom S, Payne N, Ghatei M, Edwards R. Effect of peptide YY on human renal function. Am J Physiol Renal Physiol. 1995; 268:F754–F759.

Savage A, Adrian T, Carolan G, Chatterjee V, Bloom S. Effects of peptide YY (PYY) on mouth to caecum intestinal transit time and on the rate of gastric emptying in healthy volunteers. Gut. 1987; 28:166–170. [PubMed: 3557189]

Shindler K, Roth K. Double immunofluorescent staining using two unconjugated primary antisera raised in the same species. J Histochem Cytochem. 1996; 44:1331–1335. [PubMed: 8918908]

Wade P, Westfall J. Ultrastructure of enterochromaffin cells and associated neural and vascular elements in the mouse duodenum. Cell Tiss Res. 1985; 241:557–563.

Zhang T, Brubaker P, Thompson J, Greeley G Jr. Characterization of peptide-YY release in response to intracolonic infusion of amino acids. Endocrinology. 1993; 132:553–557. [PubMed: 8093875]

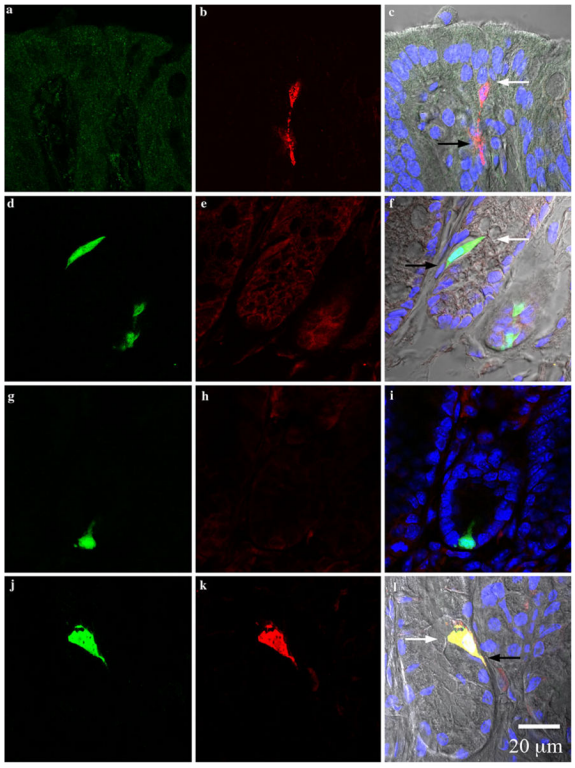

Fig. 1.

Photomicrographs from colonic crypts. All sections are aligned vertically with the lumen on top. *White* and *black arrows* point to the lumen and lamina propria, respectively. Colors represent the following: *green* green fluorescent protein (*GFP*), *red* PYY, *blue* DAPI, and *gray* differential interference contrast (*DIC*) and are merged from the left and middle columns. **a**–**c** Sections from wild type Swiss Webster mice stained for GFP (**a**) and PYY (**b**). GFP is absent and PYY cells appeared to have a spindle-like shape in the colon of wild type mice. **d**–**f** Sections from PYY-GFP mice incubated with secondary antibodies alone (DyLight488-conjugated donkey anti-chicken and Cy3-conjugated donkey anti-rabbit). Colonic cells from transgenic PYY-GFP mice expressed endogenous GFP and non-specific binding of secondary antibodies was absent. **g**–**i** Sections from a PYY-GFP mouse incubated in the presence of chicken anti-GFP and rabbit anti-PYY pre-adsorbed in excess (10 μM) of PYY peptide. The specificity of the antibody to PYY is shown by the absence of immunoreactivy after pre-absorption with synthetic PYY. **j**–**l** PYY-GFP sections incubated in the presence of chicken anti-GFP and rabbit anti-PYY antibodies. PYY immunoreactivity with the antibody exclusively co-localized with GFP positive cells (l, *yellow*). Please refer to online version of the article for colored figures

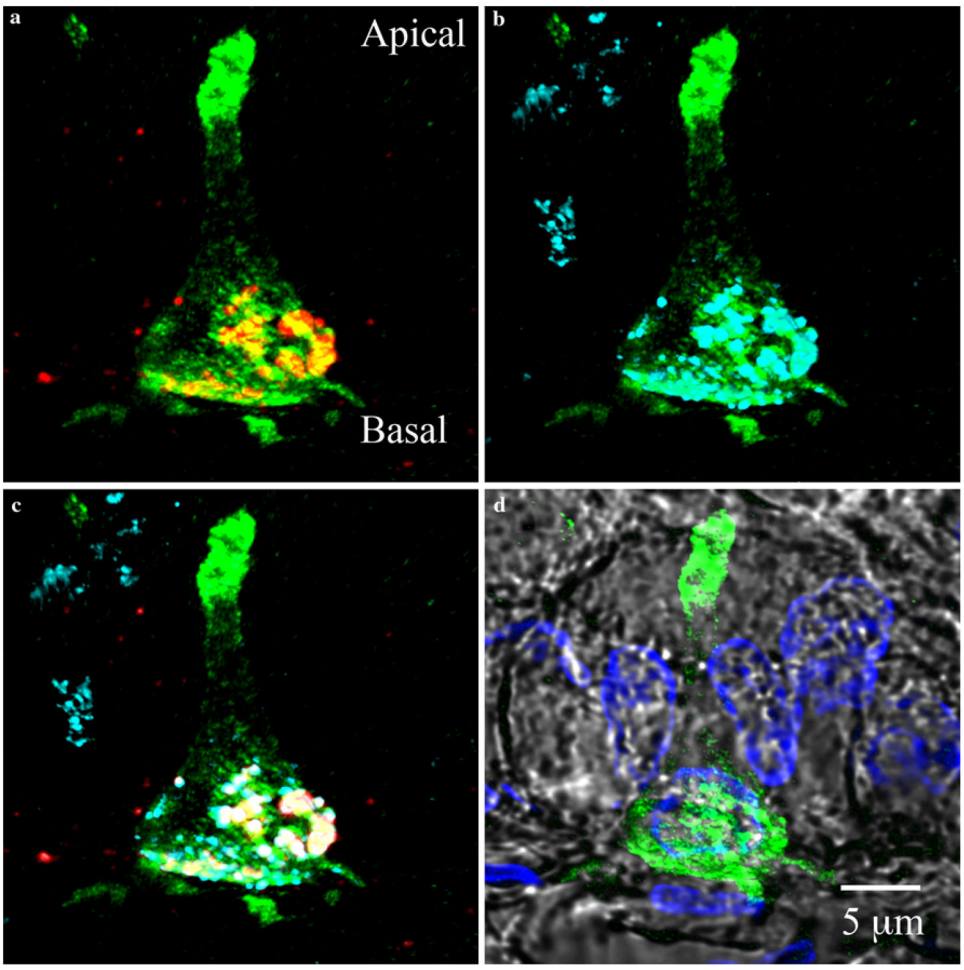

Fig. 2.

Colocalization of PYY and glucagon-like peptide 1 (*GLP-1*) in PYY-GFP cells of the ileum. **a** PYY staining (*red*) reveals confinement of granules to the basal end of the PYY-GFP cell. **b** GLP-1 staining (*cyan*) shows colocalization at the basal side of the PYY-GFP cell. **c** Image overlay of PYY and GLP-1 granules colocalized at the base of PYY-GFP cell (*green* GFP, *red* PYY, *cyan* GLP-1 and *white* overlapping of PYY and GLP-1. Staining for PYY (*red*) and GLP-1 (*cyan*) are projected as maximal intensities. Note that not all PYY and GLP-1 staining colocalizes within the same granules. This has been previously demonstrated by electron immu-nogold staining (Nilsson et al. 1991). **d** Position of PYY-GFP cell with respect to other cells of the epithelium (*green* GFP, *blue* DAPI and *gray* DIC)

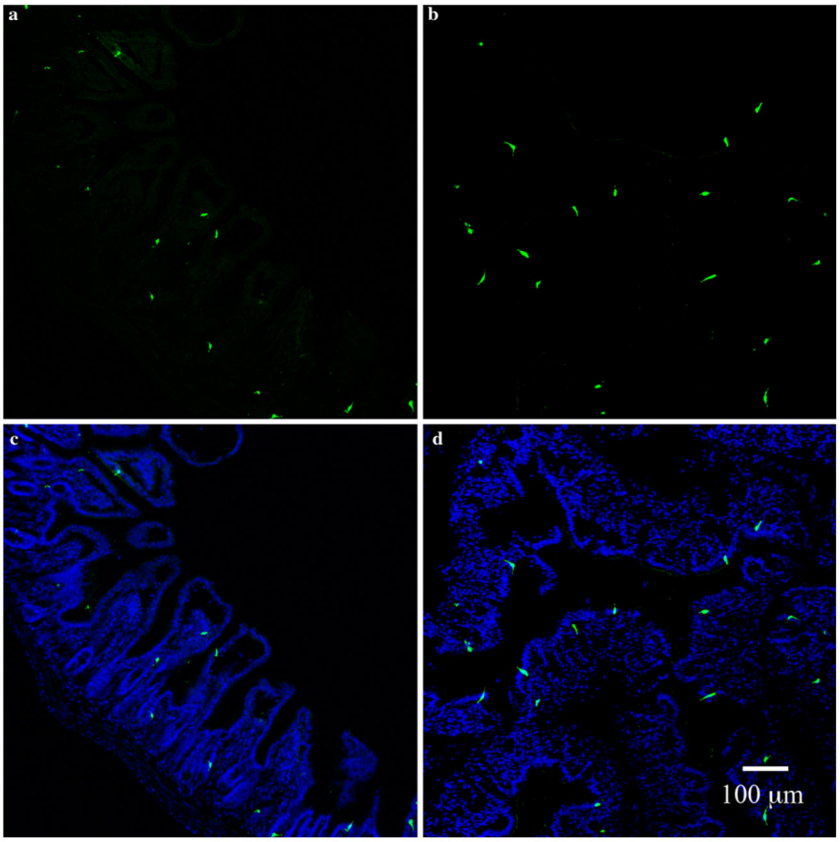

Fig. 3.

Distribution of PYY-GFP cells in the ileum and colon. Sections of ileum (**a**, **c**) and colon (**b**, **d**) from a PYY-GFP mouse stained with chicken anti-GFP (**a**, **b**) and composite with DAPI nuclei (*blue*) stain (**c**, **d**). PYY-GFP cells appear to be more abundant in the colon than in the ileum. Note the spindle-like anatomy of PYY-GFP cells in the colon compared to the L shape of those in the ileum

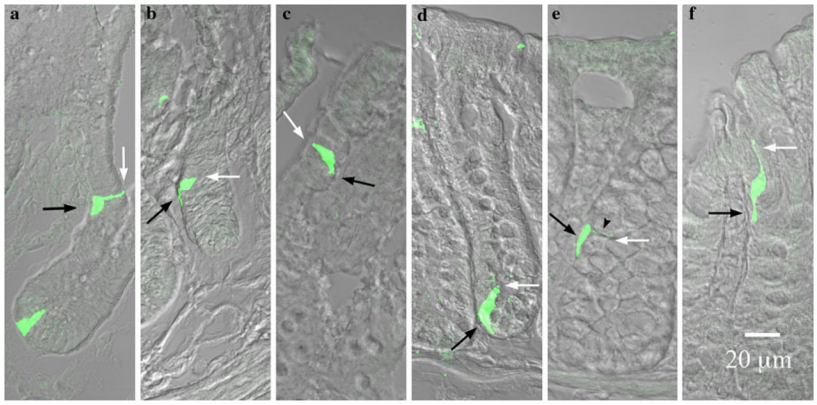

Fig. 4.

PYY-GFP cell morphology in the ileum versus colon. *White* and *black arrows* indicate the lumen and lamina propria respectively. **a–c** In the ileum a cells were columnar or flask-shaped at the bottom of the crypts and pseudopod-like basal processes were absent. Further up the crypt (**b**) towards the villus tip (**c**) basal processes became evident. **d–f** In the colon, flask-shaped cells were evident at the bottom of the crypts (**d**). A neck-like projection (*black arrow head*) and a basal process were evident in the cell in the middle of the crypt (**e**). Towards the apex of the crypt, this neck-like projection extended to maintain contact with the lumen, while the basal process remained in contact with the lamina propria (**f**). Note the sigmoidal appearance of the cell to maintain contact with the lumen as well as the lamina propria

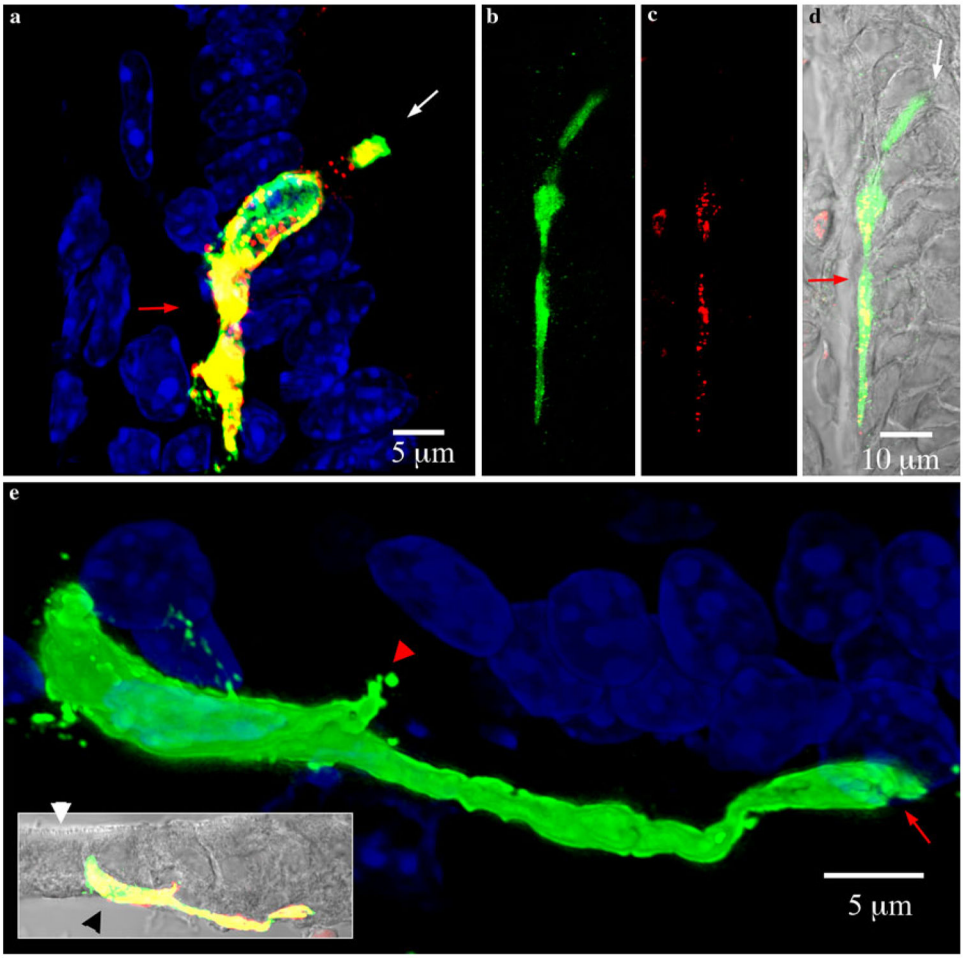

Fig. 5.

Pseudopod-like basal processes in PYY-GFP cells of the ileum. *White* and *red arrows* indicate the lumen and lamina propria respectively. Sections imaged were 15 μm thick. **a** Maximal projection view of typical PYY-GFP cell in a villus of the ileum. The pseudopod-like process runs on the basal side, in between the lamina propria and the base of other epithelial cells. The basal process typically extends downward towards the bottom of the crypt. **b**–**d** PYY-GFP cell with a long basal process extending along the base of adjacent epithelial cells. The total length of the cell is greater than 70 μm and the basal process is approximately 50 μm long. **b** *Green* GFP, **c** *red* PYY, **d** composite with DIC (*gray*). **e** Maximal projection view of PYY-GFP cell in a villus from the ileum. *Inset* shows the cell position with respect to the brush border (*white arrow head*) and lamina propria (*black arrow head*) (*green* GFP, *red* PYY staining, *yellow* merged images, *gray* DIC). The pseudopod-like basal process often ended in a bifurcation (*red arrow*). There are some smaller projections (*red arrow head*) that extended from the body of the cell

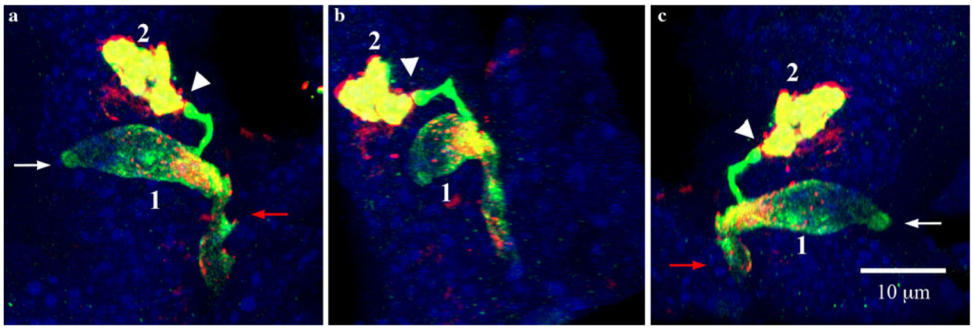

Fig. 6.

Relationship of a PYY-GFP cell with another PYY-GFP cell through synapse-like structures at the end of pseudopod-like processes. *White* and *red arrows* indicate the lumen and lamina propria respectively. Section imaged was 15 μm thick. **a**–**c** Views of three-dimensionally reconstructed PYY-GFP cells in a villus of the ileum from different angles. The synapse-like projection at the end of pseudopod-like process from cell 1 that makes contact with cell 2 is shown by the *white arrowhead. Green* GFP, *red* PYY staining, *yellow* merged images, *blue* DAPI

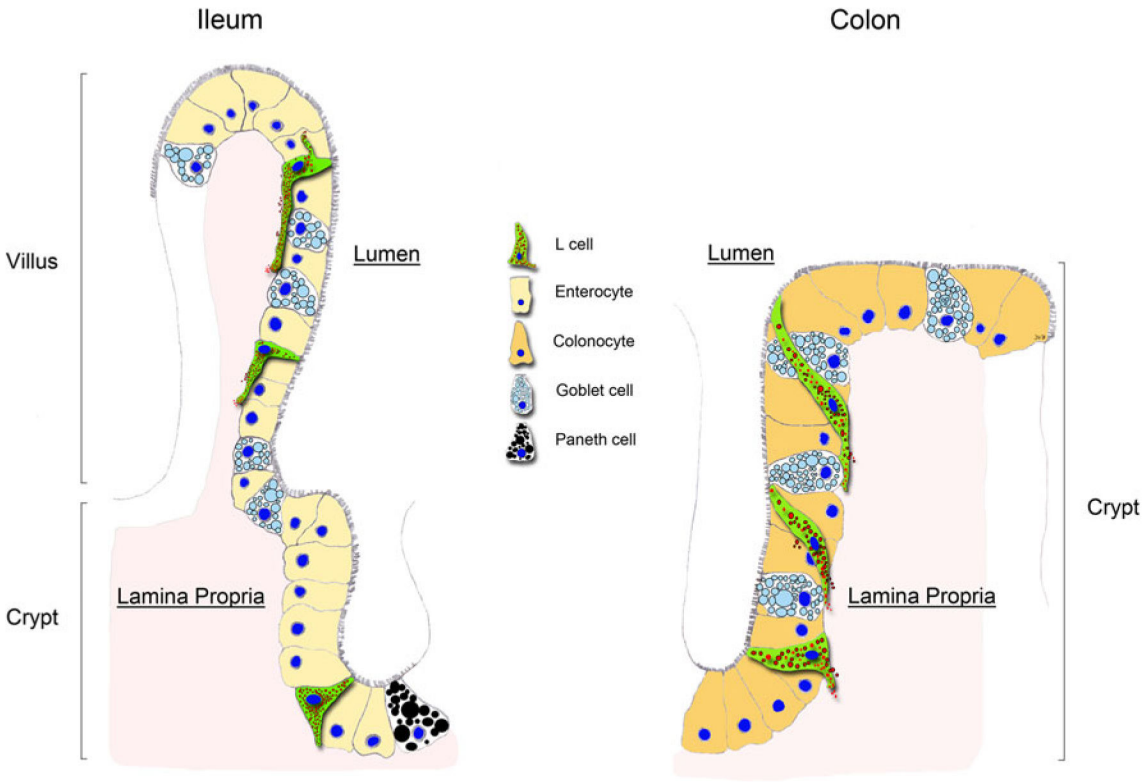

Fig. 7.

Representation of PYY cells in the ileum versus colon. In the ileum, PYY cells (L cells) are flask-shaped at the crypt whereas, in the villus, a long pseudopod-like process extends at their base. The basal processes usually extend toward the crypt. Occasionally, more than one process can extend from the body of the cells toward other epithelial cells. In the colon, PYY cells are flask-shaped at the bottom of the crypt. However, at the apex of the crypt, PYY cells weave through other epithelial cells and the tip of the cell runs along the crypt's lumen. The base of the same PYY cell runs vertically along the crypt's lamina propria. Whereas in the ileum PYY cells maintain minimal contact with the gut lumen, in the colon PYY cells appear to have a larger surface area exposed to the lumen

Table 1

Primary and secondary antibodies used in immunofluorescence analysis

Primary antibody	Species	Source	Dilution[a]	Secondary antibody	Source	Dilution
PYY (aa 4–21)	Rabbit	Biosource	1:2,000	Cy3-conjugated donkey anti-rabbit	Jackson ImmunoResearch	1:1,000
GFP	Chicken	Abcam	1:1,000	Dylight488-conjugated donkey anti-rabbit	Jackson ImmunoResearch	1:1,000

PYY peptide tyrosine tyrosine, *GFP* green fluorescent protein

[a] All antibodies were diluted in 50 mM TRIS-buffered saline containing 0.05% Tween-20 and 0.1% bovine serum albumen

Table 2

Antibodies used in immunofluorescence analysis with the Tyramide Signal Amplification (TSA™) method

Primary antibody	Species	Source	Dilution[a]	Detection method	Source	Dilution
PYY (aa 4–21)	Rabbit	Biosource	1:1,000,000	HRP-conjugated donkey anti-rabbit TSA™-Plus Cy5	Jackson ImmunoResearch PerkinElmer	1:1,000 1:200[b]
GLP-1	Rabbit	Abcam	1:500	Cy3-conjugated donkey anti-rabbit	Jackson ImmunoResearch	1:1,000
GFP	Chicken	Abcam	1:1,000	Dylight488-conjugated donkey anti-rabbit	Jackson ImmunoResearch	1:1,000

PYY peptide tyrosine tyrosine, *GLP-1* glucagon-like peptide 1, *GFP* green fluorescent protein

[a] All antibodies except for TSA™ were diluted in 50 mM TRIS-buffered saline containing 0.05% Tween-20 and 0.1% bovine serum albumen

[b] TSA™-Cy5 reagent was diluted in 1X Plus Amplification Diluent provided with the TSA™ kit (PerkinElmer, Waltham, MA)